Techniques for Noise Removal and Registration of TIMS Data

Susanne Hummer-Miller
U. S. Geological Survey, Denver, CO 80225

ABSTRACT: Extracting subtle differences from highly correlated thermal infrared aircraft data is possible with appropriate noise filters, constructed and applied in the spatial frequency domain. This paper discusses a heuristic approach to designing noise filters for removing high- and low-spatial frequency striping and banding. Techniques for registering thermal infrared aircraft data to a topographic base using Thematic Mapper data are presented. The noise removal and registration techniques are applied to TIMS thermal infrared aircraft data.

INTRODUCTION

REMOVAL OF NOISE in thermal infrared aircraft data is an important preprocessing consideration when subtle differences are to be extracted from highly correlated data. The Thermal Infrared Multispectral Scanner (TIMS) is an experimental aircraft instrument that provides six channels of thermal radiance data in the 8 to 12 micrometre region of the electromagnetic spectrum. These data contain information on surface temperature and on spectral emissivity and yield spectra diagnostic of rock-forming minerals (Watson *et al.*, 1989). The data are highly correlated (typical correlation coefficients of $r = 0.99$) because the radiance measured in each channel has a strong dependence on surface temperature. The spectral emissivity variation between channels is small compared to the temperature variation; therefore, decorrelation techniques and emissivity models are required to extract subtle emissivity differences related to different materials. Spectral emissivity is useful for mapping surface lithology and mineral alteration based on the physical properties of geologic materials (Kahle and Goetz, 1983; Kahle, 1987; Watson *et al.*, 1989). Preprocessing of these data requires experimenting with noise removal techniques for each particular data set and geometric registration to a standard base.

Daytime TIMS data used in this study are centered around the Carlin mining district in northeast Nevada and were acquired at 10:40 AM local solar time on 27 July 1983. Using a 512- by 512-element window with an average resolution of 25 m, a decorrelated image of this area was constructed to evaluate the noise removal and registration techniques.

NOISE REMOVAL

In general, TIMS data contain significant noise from various sources such as variations in detector sensitivity and microphonic vibration of the detector (Palluconi and Meeks, 1985; Gillespie, 1986). The noise is characterized by random bit dropouts, bit errors occurring when neighboring pixels have significantly different radiance values (sometimes referred to as ridge runners), and high-and low-spatial frequency striping and banding. The bit errors/dropouts are single noise pixels (single picture elements in digital space) recognizable by their relatively low digital values (usually less than 70 DN) in the raw data. This noise is removed easily by a mean-threshold filter applied one-dimensionally in the spatial domain.

For the Carlin TIMS data, the bit errors and dropouts occurred at the same location in each of the six channels. Channel six displayed an additional error/dropout pattern usually within pixels 405 to 455. A one-dimensional, mean-threshold filter was applied to test pixels values of less than 70 DN by computing a quantity that is the sum of the two neighboring values minus twice the value of the test pixel. If this quantity exceeds a predetermined level of 40, the test pixel is labeled as a bit error/dropout. The predetermined level may vary with data sets and is selected by examining several of the bit dropout areas. Once a bit error/dropout is identified, several replacement schemes can be used: a linear interpolation of the two neighboring values on the same scanline, a bilinear interpolation, or algorithms that replace a bit error with a local mean value.

A thermal radiance image, even after a mean-threshold filter has been applied, does not generally show the more subtle striping and banding noise remaining in the image data. The noise tends to be poorly correlated among channels and can be enhanced by various processing techniques. Examples of image products that enhance noise are a ratio image of two channels and more complicated decorrelated images (Taylor, 1973; Soha and Schwartz, 1978; Gillespie *et al.*, 1986). Figure 1 is the first of three bands transformed by decorrelating bands 1, 3, and 5 and shows different noise patterns, the most prominent of which

FIG. 1. A decorrelated TIMS daytime image before filtering (raw data). This image is the first of three bands transformed by decorrelating bands 1,3,5 and is centered on the Carlin Gold Mine (dark area) in northeastern Nevada. Scanline striping and variable diagonal banding are evident.

PHOTOGRAMMETRIC ENGINEERING AND REMOTE SENSING,
Vol. 56, No. 1, January 1990, pp. 49-53.

0099-1112/90/5601-49$02.25/0

are the along-scanline striping and the diagonal, variable-width banding.

The coordinate systems used in this analysis are shown in Figure 2. In the spatial domain, x is the pixel location along a scanline, and y is the pixel location for increasing scanlines along the flight direction. Figure 2c is one representation of the Fourier (frequency) domain. Quadrant I has the DC point at zero frequency location, and the directions of the x and y frequencies for each quadrant are noted. The symmetry in this domain is such that quadrant III is flipped and reversed from quadrant I. Similarly, quadrants II and IV are flipped and reversed from each other. The folding or Nyquist frequencies (f_{Nx}, f_{Ny}) are indicated. For building filters in the Fourier domain with this representation of the transform, the variables u and v are used as defined in Figure 2b.

A two-dimensional, fast Fourier transform (2D-FFT) algorithm was applied to a decorrelated image (Figure 1), and the resulting image of the transform, a logarithmic presentation of the power spectrum, is shown in Figure 3. The transform is a matrix of values the higher of which are centered around the zero frequency point (DC location), preserving the symmetry of the four quadrants. The DC term contains the majority of the information content of the scene and was reduced in this image, compressing the dynamic range so that the entire transform could be seen. Noise patterns in the spatial domain are expressed in the Fourier domain as bright patches at angles orthogonal to spatial noise patterns (Figure 3). Because of the symmetry of the transform, only quadrants I and IV need be examined. Filters built in these quadrants can automatically be reflected into the other two.

A heuristic approach was used to design filters that would

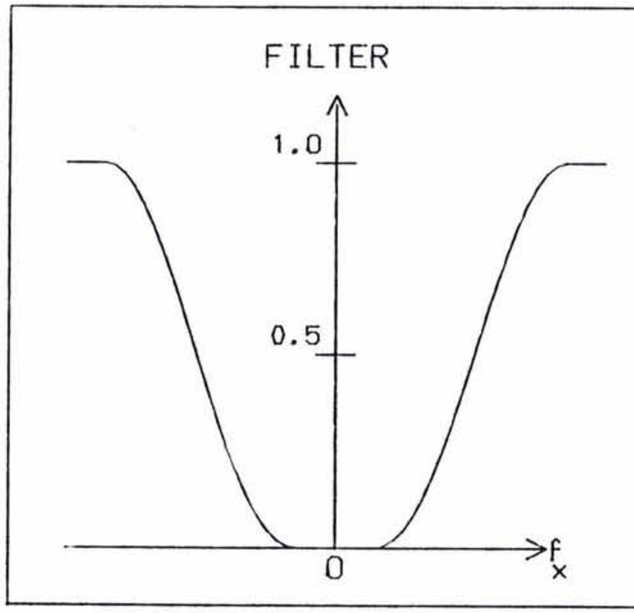

FIG. 3. A logarithmic presentation of the Fourier transform power spectrum on Figure 1. The transform representation is defined in Figure 2(c).

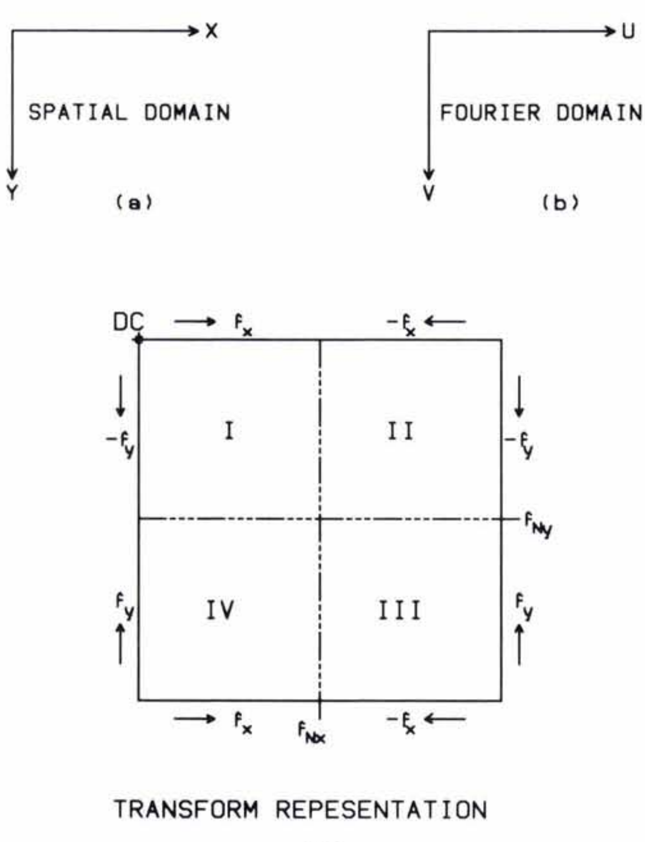

FIG. 2. The coordinate systems used in this analysis for (a) the spatial domain, (b) the Fourier domain, and (c) the transform representation.

multiply the transform to pass or reject data. A filter is a matrix of numbers ranging from zero to one which multiply the value of the transform at every location. A filter value of one leaves the transform value unchanged; a filter value of zero changes the transform value to zero. A rounded edge filter will have values gradually decreasing from one to zero. Appropriate rounding of filter edges is necessary to avoid introducing artifacts (Peli and Verly, 1983) and becomes more important the closer the filter is to the DC term where the transform values are the highest and rapidly changing. All rounded filters used in this analysis employed a $\sin(b)/b$ type of smoothing.

A "bathtub" filter (Figure 4) was constructed to remove the major low f_y spatial frequency, along-scanline noise. As the name implies, the filter is elongated in the vertical (v) direction with rounded edges (A in Fig. 5). The symmetry is such that the center and half the bathtub are on the left-hand side of the figure and the other half is reflected on the right-hand side. The u and v parameters are the starting positions for the filter to smooth from a value of 1 to 0 over a 6-pixel range. Many bathtub filters were constructed with various u and v parameters. These filters were applied individually to the transform and the inverse 2D-FFT was performed. The effects of the filters were visually evaluated on the resulting images to determine the best choice of parameters. For the Carlin data, the u position was chosen as 8 and the v position as 10.

Further examination of quadrants I and IV of the transform (Figure 3) shows obvious bright, vertical stripes due to high f_y frequency, along-scanline noise. These noise stripes have variable widths (v range) and their u locations are not necessarily multiples of one another. Sharp blocking filters (i.e., no rounding of filter edges) were constructed to obscure these stripes. Two methods were used to build these filters. The first was to set the filter value to 0. The second was to smooth across these stripes with non-zero values. One method was not noticeably better than the other for the Carlin data. The three sharp blocking filters used have a v range of 1 to 512. The u ranges are 79 to 82, 158 to 164, and 188 to 192. The filters are reflected in quadrants II and III.

The bathtub and sharp block filters (B's in Figure 5) were then

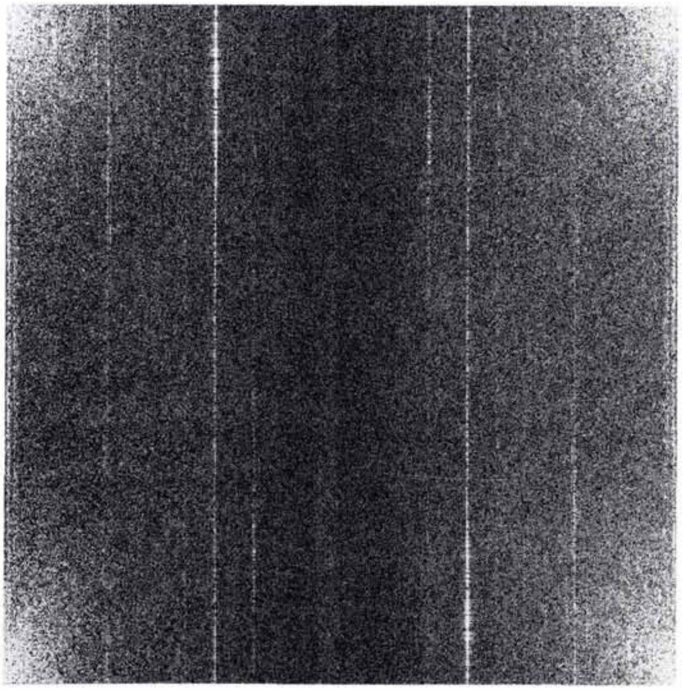

FIG. 4. A cross-section of a bathtub filter. The filter is smoothed from 0 to 1.

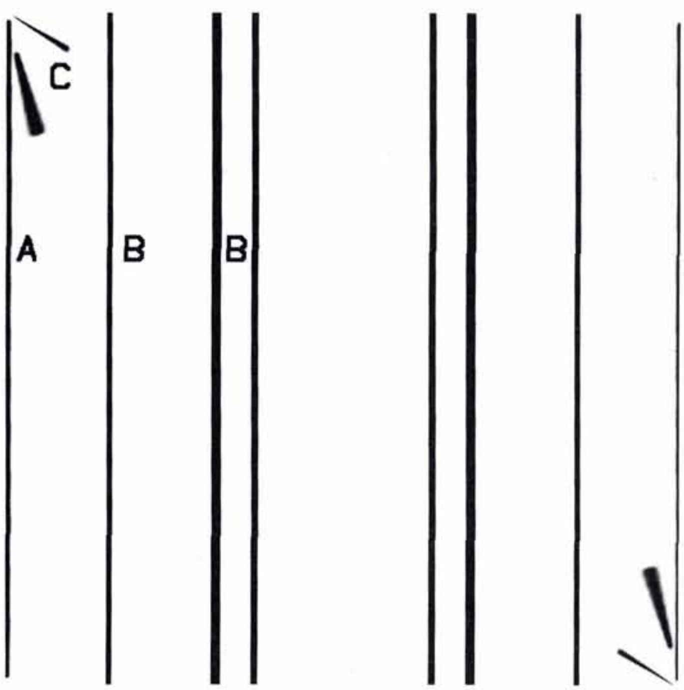

FIG. 5. An image of the filter built in the Fourier domain to be applied to the transform. The composite filter consists of a (1) bathtub (A), (2) several sharp blocking filters (B), and (3) two rounded, angular wedges (C). Note the symmetry of the filter for the four quadrants.

combined into a single filter matrix and applied to the transform. The resulting inverse transform image showed that the majority of the along-scanline noise had been removed. At this stage, the major noise patterns are diagonal to the scanline.

The angle of the diagonal noise with respect to the scanline and the frequency of the banding were estimated from the decorrelated image (Figure 1). An angular wedge filter (C in Figure 5) was constructed to match these parameters and the edges of the filter was rounded. Again, various types of angular wedges, both sharp and rounded, were tried and visually evaluated. The Carlin data required two angular wedge filters that have values 0 to less than 1. The first has an angle of $32 \pm 10°$ with a radius of 5 to 60; the other has an angle of $75 \pm 15°$ with a radius of 30 to 100. A final composite filter of (1) the bathtub, (2) sharp blocking, and (3) rounded angular wedge filters was then constructed and applied to the transform (Figure 3). The inverse 2D-FFT was performed and the resulting, filtered image is shown in Figure 6. Visually comparing the filtered and unfiltered images, a majority of the noise has been removed and no additional artifacts appear to have been introduced. The composite filter can now be applied to all of the original bands.

GEOMETRIC REGISTRATION

A variety of registration techniques are available, the choice of which is dependent upon the type of data and upon the geometric distortions present due to the stability of the acquisition platform (Bernstein, 1983). Because thermal infrared data are a measure of the surface temperature, the data appear fundamentally different from reflectance data (e.g., cultural features, such as road intersections and towns which have sharp boundaries on reflectance data and on topographic maps, may have at most tonal pattern variations on thermal data). Several registration techniques have been employed (Watson *et al.*, 1982; Price, 1982; Watson *et al.*, 1984; Hummer-Miller, 1989) for registering thermal data to base maps utilizing a broad-band reflectance channel that was simultaneously acquired.

TIMS data have no accompanying reflectance channel to facilitate registration to a topographic base map, and initial registration using only thermal data proved inaccurate. Therefore, a two-step registration scheme was devised that employs Thematic Mapper (TM) satellite reflectance data. The TM scene (30-m resolution) selected was acquired with similar illumination

FIG. 6. The daytime decorrelated TIMS image after the filter in Figure 5 was applied to Figure 1.

geometry (approximately 10:00 local solar time) and in the same season (16 July 1984) as the TIMS (25-m resolution). Because the resolutions are so similar, only a 512- by 512-pixel TM window was required to match the TIMS coverage.

Using a video display device, features were selected on the TM image and the corresponding control point was marked on a 1:24,000-scale topographic map of the Rodeo Creek, NE quadrangle. The Landsat TM satellite is a relatively stable acquisition platform that introduces only minimal geometric distortion. A simple affine transformation (translation, rotation, skew, contraction, or expansion with respect to a fixed origin) using less than ten control points is adequate for the geometric registration to the map base. Nearest neighbor resampling was used, preserving the 30-m resolution. The registered, digital TM scene is the base to which the thermal aircraft data were geometrically corrected. The TM scene, in addition to displaying sharp cultural and topographic features, presents a tonal display that roughly approximates the tonal variation in the thermal data.

Aircraft data generally require a complex registration scheme because of the random motion during flight and systematic distortions like panoramic distortion and parallax displacement in rugged terrain. Although gyroscopic compensation can help reduce the distortion introduced by the roll of the aircraft, the distortion resulting from other maneuvering motions requires a non-linear transformation correction. The TIMS data were first roughly registered to the geometrically-corrected TM scene by selecting a few (less than ten) control points and applying a simple affine transformation. Using a video display device, control points were selected on the TM image and the corresponding points on the rough registered TIMS image. For this method, a roughly uniform grid of control points with a higher density of points in areas of greatest distortion is required. Reflectance data appear different from thermal data; however, some features, such as road intersections, water bodies, and changes in topography, are still recognizable by tonal pattern variations, even if they appear reversed in brightness.

A non-linear transformation was employed that involves using the four nearest control points for determing the correction at any location (x,y). First, for each selected control point, a correction in the x direction (DELX) and a correction in the y direction (DELY) are determined; i.e.,

$$\mathrm{DELX}_i = x(\mathrm{TM})_i - x(\mathrm{TIMS})_i \tag{1}$$

$$\mathrm{DELY}_i = y(\mathrm{TM})_i - y(\mathrm{TIMS})_i \tag{2}$$

where $i = 1$, total number of control points.
For any pixel location (x,y), the square of the distances (DSQ) to the four nearest control points are determined by

$$\mathrm{DSQ}_i = (x_i - x)^2 + (y_i - y)^2. \tag{3}$$

The x correction (XCOR) to be applied to any point (x,y) is a weighted mean of the inverse distance of the four nearest control points times the correction at each of the control points; i.e.,

$$\mathrm{XCOR} = \sum_{j=1}^{4} \frac{\mathrm{DELX}_j * (\mathrm{DSQ}_j)^{-1}}{\left(\sum_{k=1}^{4} (\mathrm{DSQ}_k)^{-1}\right)} \tag{4}$$

where j,k = four nearest control points.
A y correction for any point (x,y) is determined in an analogous manner. The resampling is done using nearest neighbor.

The accuracy of the registration was evaluated by rapidly switching between the TM and the TIMS on a video display device and noting spatial movement of corresponding points between the two images. If distortion still is evident in certain areas, more control points can be added from the rough-registered TIMS image and the transformation can be repeated.

EVALUATION OF RESULTS

For further evaluation of the effectiveness of the noise removal and the accuracy of the registration, two additional products were used: a digital image of the topographic map and a digital image of the geologic map (Evans, 1974) (1:24,000 scale). The image maps are from mylar separates without cultural features. High-quality black-and-white prints were produced from the separates and scanned with a digital camera at a resolution of 5 metres per digital element. Lines from the two digital image maps were converted to binary form and digitally superimposed on both the TM and TIMS images.

Figure 7 is TM band 3 with the topography superimposed. The accuracy of the registration is evident by the coincidence of the stream beds, mountain ridges, and mountain peaks with the contour lines.

Figure 8 is the first of three bands transformed by decorrelating TIMS bands 1, 3, and 5 and has been noised filtered and geometrically registered to the topographic base using the TM image. Superimposed on the decorrelated image (Figure 8) is the digitized, geometrically-registered geologic map. The noise present in Figure 1 appears to be suppressed in Figure 8, and coincidence of the geologic unit boundaries with various tonal patterns indicates the accuracy of the registration. A discussion of extracting the spectral emissivity using these TIMS data and

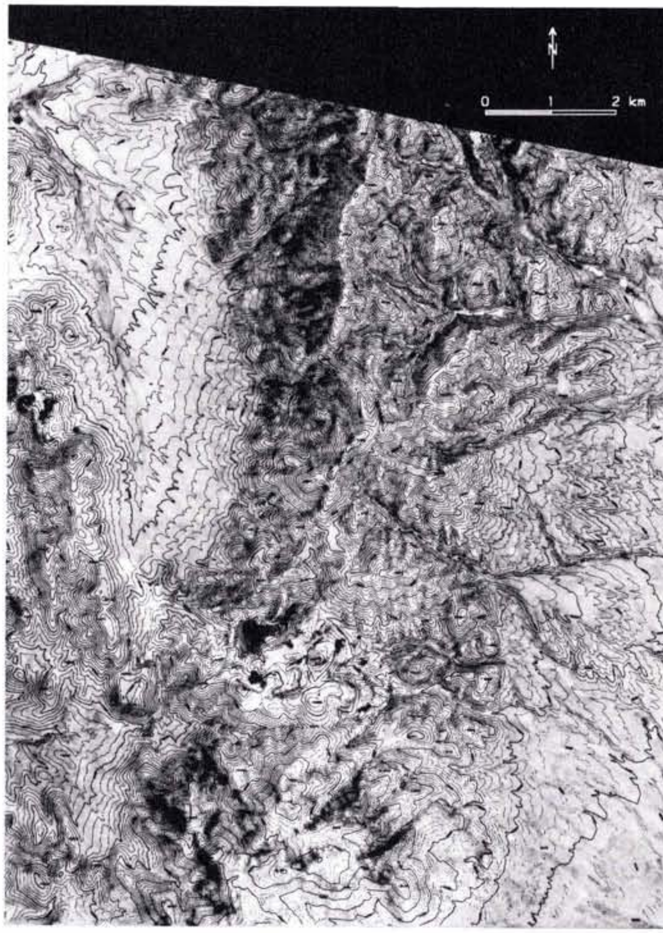

FIG. 7. A TM image (band 3) with the topography digitally superimposed. The area is almost the entire 1:24,000-scale map of Rodeo Creek, NE, Eureka County, Nevada.

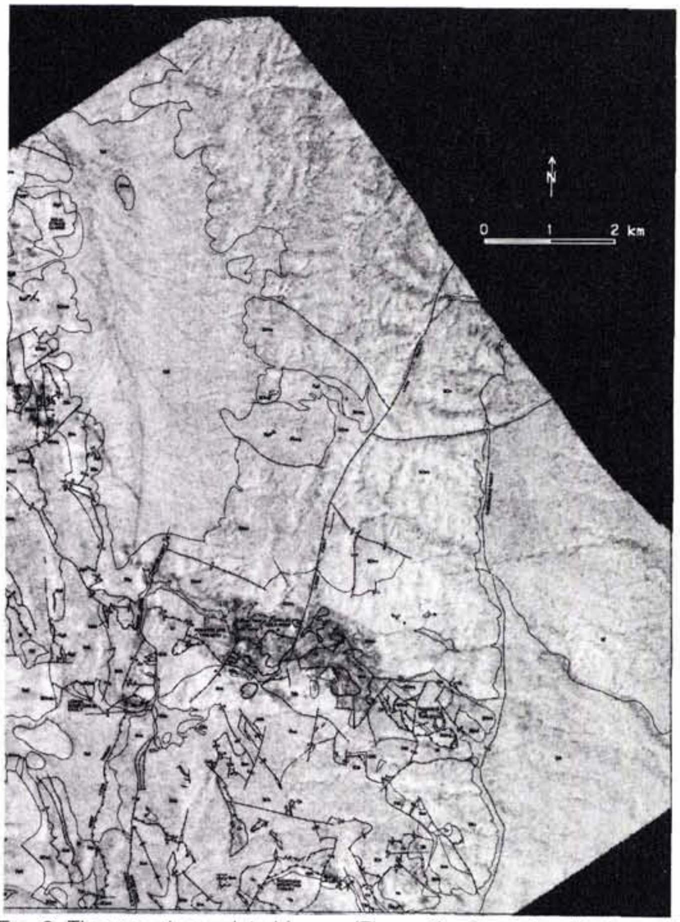

FIG. 8. The TIMS decorrelated image (Figure 6), after noise filtering and registration, with the geology digitally superimposed to show the accuracy of the registration.

their association with the geologic units is presented with color illustrations in Watson *et al.* (1989).

SUMMARY

The techniques presented are applicable to any remotely sensed data set and are particularly useful for aircraft data. It is not necessary to determine the sources of the noise, just the frequency characteristics. For a quick-look analysis, a noise filter similar to the one presented here (using a bathtub, sharp blocking and angular wedges) was applied to another TIMS data set with results similar to the Carlin data. This suggests that, once an effective noise filter has been constructed for a particular instrument, it is highly probable that refinements to that filter are all that may be necessary for other data sets from that instrument.

The registration techniques presented were developed for thermal infrared data with no accompanying reflectance channel. The results show that, with the inclusion of TM reflectance data, the thermal data can be accurately geometrically corrected. For aircraft data with a reflectance channel, the registration techniques will be even easier to use.

ACKNOWLEDGMENTS

The author acknowledges Ken Watson for his help in developing these techniques.

REFERENCES

Bernstein, Ralph (ed.), 1983. Image Geometry and Rectification, *Manual of remote sening*, 2d Ed., Vol. I, Chapter 21, Theory, Instruments and Techniques (edited by D. S. Simonett and F. T. Ulaby): Falls Church, Virginia, American Society of Photogrammetry, pp. 873–922.

Evans, J. G., 1974. *Geologic Map of the Rodeo Creek NE Quadrangle, Eureka County, Nevada*, U.S. Geological Survey Geologic Quadrangle Map GQ-1116, 1:24,000 scale.

Gillespie, A. R., 1986. Enhancement of TIMS Images for Photointerpretation, *The TIMS Data User's Workshop* 18 and 19 June 1985, Jet Propulsion Lab. Publication 86-38, pp. 12–24.

Gillespie, A. R., A. B. Kahle, and R. E. Walker, 1986. Color Enhancement of Highly Correlated Images. I. Decorrelation and HCI Contrast Stretches, *Remote Sensing of Environment*, Vol. 20, pp. 209–235.

Hummer-Miller, Susanne, 1989. A Digital Mosaicking Algorithm Allowing for an Irregular Join "Line," *Photogrammetric Engineering and Remote Sensing*, Vol. 55, No. 1, pp. 43–47.

Kahle, A. B., 1987. Surface Emittance, Temperature, and Thermal Inertia Derived from Thermal Infrared Multispectral Scanner (TIMS) Data for Death Valley, California, *Geophysics*, Vol. 52, No. 7, pp. 858–874.

Kahle, A. B., and A. F. H. Goetz, 1983. Mineralogic Information from a New Airborne Thermal Infrared Multispectral Scanner, *Science*, Vol. 222, No. 4619, pp. 24–27.

Peli, T, and J. G. Verly, 1983. Digital Line-artifact Removal, *Optical Engineering*, Vol. 22, No. 4, pp. 479–484.

Palluconi, F. D., and G. R. Meeks, 1985. *Thermal Infrared Multispectral Scanner (TIMS): An Investigator's Guide to TIMS Data*, Jet Propulsion Lab. Publication 84–32, 25p.

Price, J. C., 1982. Registration of Heat Capacity Mapping Mission Day and Night Images: forum, *Photogrammetric Engineering and Remote Sensing*, Vol. 48, No. 9, pp. 1466–1467.

Soha, J. M., and A. A. Schwartz, 1978. Multispectral histogram normalization contrast enhancement, *Proc. 5th Canadian Symposium on Remote Sensing*, Victoria, BC, Canada, pp. 86–93.

Taylor, M. M., 1973. Principal components color display of ERTS imagery, *Third Earth Resources Technology Satellite-1 Symposium*, 10-14 December, NASA SP-351, Vol. 1, Section B, pp. 1877–1897.

Watson, K., Susanne Hummer-Miller, and D. L. Sawatzky, 1982. Registration of Heat Capacity Mapping Mission Thermal Satellite Images, *Photogrammetric Engineering and Remote Sensing*, Vol. 48, No. 2, pp. 263–268.

Watson, K., Susanne Hummer-Miller, D. H. Knepper, Jr., M. D. Krohn, M. H. Podwysocki, H. H. Pohn, G. L. Raines, and L. C. Rowan, 1984. *Application of Heat Capacity Mapping Mission Data to Regional Geologic Analysis for Mineral and Energy Resource Evaluation*, National Technical Information Service, N84-16625, 120 p.

Watson, K., F. A. Kruse, and Susanne Hummer-Miller, 1989. Thermal infrared exploration in the Carlin Trend, northern Nevada (submitted to *Geophysics*).